*Microcirculation*, 16: 559–571, 2009

ISSN: 1073-9688 print / 1549-8719 online
DOI: 10.1080/10739680902956107

informa
healthcare

# Time Development Models for Perfusion Provocations Studied with Laser-Doppler Flowmetry, Applied to Iontophoresis and PORH

FRITS F.M. DE MUL,* JUDITH BLAAUW,† RIES J. SMIT,‡ GERHARD RAKHORST,* AND JAN G. AARNOUDSE†

University of Groningen, Faculty of Medicine, Departments of *Biomedical Engineering BMSA; †Obstetrics and Gynecology; ‡Internal Medicine, University Medical Center Groningen, Groningen, The Netherlands

ABSTRACT

**Objective:** Clinical acceptance of laser-Doppler perfusion monitoring (LDPM) of microcirculation suffers from lack of quantitatively reliable signal data, due to varying tissue constitution, temperature, hydration, etc. In this article, we show that a novel approach using physiological models for response upon provocations provides quantitatively and clinically relevant time constants. **Methods:** We investigated this for two provocation protocols: postocclusive reactive hyperemia (PORH) and iontophoresis shots, measured with LDPM on extremities. PORH experiments were performed on patients with peripheral arterial occlusive disease (PAOD) or diabetes mellitus (DM), and on healthy controls. Iontophoresis experiments were performed on pre-eclamptic patients and healthy controls. We developed two dynamical physical models, both based on two characteristic time constants: for PORH, an ''arterial'' and a ''capillary'' time constant and, for iontophoresis, a ''diffusion'' and a ''decay'' time constant. **Results:** For the different subject groups, we could extract time constants that could probably be related to physiological differences. For iontophoresis, a shot saturation constant was determined, with very different values for different groups and administered drugs. **Conclusions:** With these models, the dynamics of the provocations can be investigated and quantitative comparisons between experiments and subject groups become available. The models offer a quantifiable standard that is independent of the type of LDPM instrumentation.
*Microcirculation* (2009) **16,** 559–571. doi:10.1080/10739680902956107

KEY WORDS: PORH, postocclusive reactive hyperemia, PAOD, peripheral arterial occlusive disease, diabetes mellitus, iontophoresis, pre-eclampsia, laser Doppler perfusion monitoring, LDPM

## Laser-Doppler Perfusion Monitoring (LDPM) of Microcirculation

LDPM measures the average blood perfusion in small vessels. It is mainly applied to monitor cutaneous blood perfusion. Coherent light from a laser partly scatters in moving red blood cells, before emerging at the tissue surface. Due to the Doppler effect, the frequency of the light will slightly change, according to the velocity of the cells. A photodiode, measuring both the original laser light and the Doppler-shifted emerged light, will produce a Doppler frequency signal. The strength and frequency content of this signal depend on the moving blood cell flow [17]. This signal can only be expressed in terms of experimental ''perfusion units'' and cannot easily be related to signal intensity (SI) units of flow. Therefore, quantitative comparisons of flow signals remain difficult, even under standardized baseline or provocation conditions.

Until now, almost all LDPM research with provocation tests has exclusively concentrated on the relative height of the excess perfusion signal, compared with that of the flux in resting conditions (the ''resting flux''). Several researchers [5,11,14] have derived some characteristics of the signal directly from reading the time plots, such as the apparent maximum of the excess signal as a function of time, and the corresponding time point of occurrence, together with the time points of half-maximum signal strength, and investigated the significance of

*Address correspondence to Frits F.M. de Mul, University of Groningen, Faculty of Medicine, Department of Biomedical Engineering BMSA, University Medical Center Groningen, P.O. Box 196, 9700 AD Groningen, The Netherlands. E-mail: fjfm@demul.net*

*Received 29 December 2008; accepted 8 April 2009.*

differences in these data over several groups of subjects (i.e., patients, healthy controls). However, since they did not use underlying explaining models, their comparisons were purely phenomenological. On the other hand, when comparing time recordings of various groups of patients and healthy (control) persons, we observed differences in the full shape of the time recordings. Therefore, it appears worthwhile to investigate these dynamical shape differences more thoroughly, and for that purpose, to quantify the characteristics, we need a physically sound model.

The functional anatomy of the microcirculation is not the same for all tissues, but basically shows the following structure. Blood enters the capillary bed through a small arteriole, which divides in several metarterioles before entering the capillaries. The musculature of the arterioles and metarterioles together with the precapillary sphincters determine, to a large extent, local tissue blood flow by contraction or relaxation. The degree of contraction of these muscular elements of the microvascular system is regulated in a complex manner. Local metabolism, endothelial activity, autocrine and paracrine pathways, and the autonomic nervous system play a major regulatory role. It is beyond the scope of this article to provide an extensive description of these regulatory systems. The functional anatomy of the skin is characterized by a superficially located network similar to the usual nutritive microvascular architecture and a subcutaneous network, consisting of an extensive venous plexus. In some areas of the skin, the venous plexuses are directly connected to the arteries by arteriovenous anastomoses. These anastomoses are relatively large vessels with strong muscular coats, controlling inflow in the venous plexuses. Constriction or relaxation of these anastomoses is regulated by the autonomic nervous system. In this way, the vascular system of the skin plays a key role in thermoregulation of the body [018].

Two types of provocation tests are frequently used in perfusion studies: postocclusive reactive hyperemia (PORH) and iontophoresis. We will use these two provocation protocols to discuss dynamical models for the time recordings of the LDPM signals.

## PORH

PORH refers to the increase in skin blood flow above baseline levels, following the release of an arterial occlusion. It is applied as a test to assess microvascular endothelial function. LDPM allows one to measure the response by measuring flow changes in the skin. PORH produces a characteristic signal output, similar to that shown in Figure 1. Upon occlusion, the blood perfusion drops from its resting flux value to the biological zero level [21]. After releasing the cuff, the blood perfusion returns to the resting flux value, but with an initial overshoot. The magnitude and time regime of this overshoot are clinically relevant diagnostic variables [05,13]0. The reason for this overshoot, especially in normal (i.e., healthy) cases, is vasodilatation due to metabolic factors resulting from the preceding ischemia and the subsequent flow-mediated vasodilatation, which is the result of the increased shear stress on the endothelium. When proximal stenosis or obstruction (i.e., atherosclerosis) is present (PAOD), the flux rise after occlusion is much slower and the peak perfusion value may be relatively lower. In case of critical ischemia, the maximum vasodilatation has already been reached in the resting period, before occlusion, and the PORH response will not show a significantly higher response than that resting flux level. The presence of stenosis in the larger arteries or flow through collaterals may cause a slower, smaller increase of flux after occlusion, which will inhibit a rapid refilling of the arterial segments. The slow rate of flux increase just after cuff release PAOD may be due to a higher resistance of the larger arterial blood vessels and the volume increase of the (larger) arterial blood vessels distal to the occlusion cuff, which determine the refill of that blood-vessel segment. The decreased rate of flux increase just after cuff release is not explained by

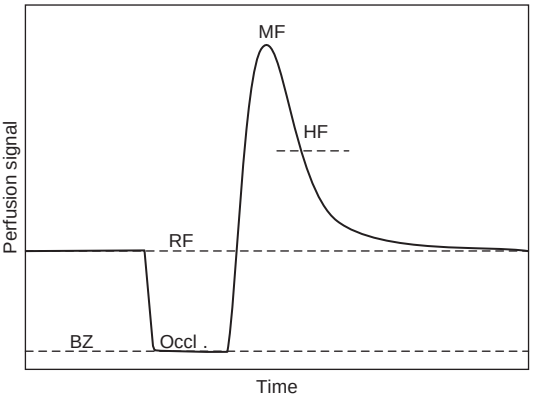


**Figure 1.** Postocclusive reactive hyperemia (PORH) response. BZ, biological zero; Occl., occlusion period; RF, resting flow; MF, maximum; HF, time of halfway decrease between maximum and resting flux.

decreased dilatation of the blood vessels. After the flow has reached its maximum value, the oxygen debt of the tissue will be absolved, and the need for the hyperemic response vanishes. At that time, the vasodilatation will decrease.

### Iontophoresis

In addition, microcirculation perfusion can be stimulated by pharmacological modulation of endothelial function, using substances such as sodium nitroprusside (SNP) or acetylcholine chloride (ACh). The first is considered to act in an endothelium-independent way, in that it directly produces nitric oxide (NO), resulting in vascular smooth muscle relaxation and thereby in vasodilation, while the second is endothelium dependent: An endothelial reaction is needed to produce NO and the described subsequent effects in the vessel wall. These substances can be administered from outside the tissue by using iontophoresis.

Iontophoresis is the introduction of charged substances into the skin by means of a small electrical current. It is based on the principle that a charged molecule migrates under the influence of an applied electrical field toward electrodes of opposite charge, placed on tissue. Generally, one electrode consists of a conductive sponge, containing the material to be introduced. The other electrode is located at some distance from the first one. A comprehensive review of the method, together with pharmaceutical, physiological, and experimental details, has been published by Banga [1]. The combination of LDPM and iontophoresis offers an opportunity to assess changes in the cutaneous microcirculation after the administration of vasoactive drugs without systemic effects. The methodology for using iontophoresis and laser-Doppler flowmetry has been widely used to investigate microvascular function in various vascular disease states, most commonly in diabetes mellitus [16,19].

Endothelial activation or dysfunction may play an important role in the clinical manifestations and pathophysiology of pre-eclampsia, a serious pregnancy complication characterized by hypertension, proteinuria, increased peripheral resistance, and reduced organ perfusion. Using iontophoresis and laser-Doppler flowmetry, increased responses of acetylcholine were found in pre-eclampsia, compared to normotensive, women [4]. We previously showed that even six to seven months after delivery, ACh-mediated reactivity was observed to be increased in women with a history of early-onset pre-eclampsia [2].

A typical time recording of an LDPM measurement during the iontophoresis process of injection is shown in Figure 2. The measurement starts with a recording of the resting flux. This is followed by a series of "shots," in which the electrical current is applied in the form of short pulses. The result is an enhanced perfusion signal, climbing to a maximum value. After the shots, the perfusion signal eventually returns to the resting flux value.

In the provocation tests, the measured values of the LDPM-signal strength have only a relative importance, due to large person-to-person variations. Therefore, we investigated the dynamical behavior of the LDPM signals as functions of time. We developed dynamic models [7,6] that can be described in terms of two time constants: for the PORH model, an "arterial" and a "capillary" time constant and, for the iontophoresis model, a diffusion and a decay time constant. The PORH model is an analog to an electrical double RC circuit (resistance and capacitance or compliance), and the iontophoresis model combines monodimensional diffusion of the pharmacological substance into the skin with decay (due to removal or saturation). These two time constants are independent of the strengths of the resting and the excess flux. Therefore, they are well suited to describe LDPM data in a universal way, independent of instrument, subject, or experimental conditions.

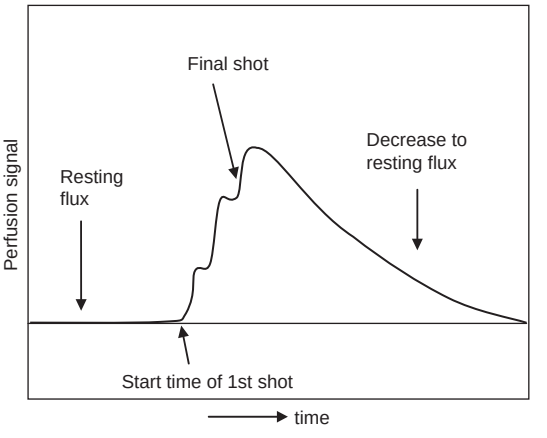


**Figure 2.** Typical time recording of an iontophoresis provocation with three "shots," as measured with laser-Doppler perfusion flowmetry.

## THE MODELS

The mathematical/physical background of the models for PORH and iontophoresis were discussed in [7,6]. Therefore, here, we concentrate on clinical measurements and discuss the models more qualitatively, using some graphics of their time development.

### The PORH Model, with Arterial and Capillary Time Constants

The physiological model for PORH [7], as described in the Introduction, should account for time-varying flow in both the "arterial" and the "capillary" parts of the circulation (see Figure 3 and Appendix).

*"Arterial" Part.* We assume that immediately after releasing the cuff after an arterial occlusion, the arterial impedance is small and the vessels are filled gradually, upon which the impedance will increase up to the level of complete filling. Then, the pressure at the entrance of the capillary part will increase gradually as well.

*"Capillary" Part.* The capillary impedance is assumed to have the following characteristics: 1) At the end of the occlusion, when releasing the cuff, the resistance of the capillaries should be small, since the arterioles are assumed to be wide open; 2) during the hyperemia period, the increased diameters of the arterioles will, subsequently, decrease and thus the resistance gradually should increase; 3) there should be a parallel "leakage" resistance to account for probable shunts inside or outside the capillary bed; and 4) finally, the resistance eventually should return to the value it had before the occlusion (i.e., the "resting flux" situation).

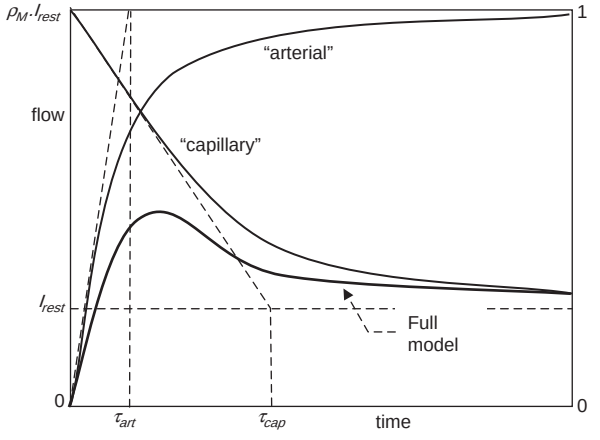


**Figure 3.** The PORH model, with the "arterial" part and the "capillary" part on the right and left vertical scales, respectively. The full model combines both parts. The two time constants, $\tau_{art}$ and $\tau_{cap}$, represent the initial slopes of the two curves. $I_{rest}$ is the resting flux level. $\rho_M$ is a factor accounting for the maximum signal level.

We used an electrical circuit analog and calculated the jump response to an instantaneous potential change, analogous to the pressure jump after releasing the cuff. In Figure 3, we have sketched the model. Both parts, "arterial" and "capillary," when treated independently, have an exponential behavior, with characteristic times, which we defined as the "arterial" time constant $\tau_{art}$ and the "capillary" time constant $\tau_{cap}$, representing the respective initial slopes. These time constants account for the arterial flow resistance and compliance (or stiffness) and for the time-dependent resistance of the local microcirculation, respectively. The "arterial" part starts from zero and saturates at unity, while the "capillary" part starts from unity (apart from a factor accounting for the signal strength) and decreases to the resting flux value. It turns out that these characteristic times help to describe the dynamic behavior of PORH, even when the overall signal strengths are varying (as is frequently the case with clinical measurements). Increasing the time constants causes the functions to broaden.

As is shown in the Appendix, the time constants, $\tau_{art}$ and $\tau_{cap}$, are inversely proportional to Young's elasticity modulus, and to the (average) vessel diameter and the wall thickness, and may, therefore, provide an indication for vasodilation or obstruction.

In [7], we described the model in detail, with its exact solution, and with an approximated solution obtained by treating the two parts as being independent. The latter is only applicable when the "arterial" part develops much faster than the "capillary" part (if $\tau_{art} << \tau_{cap}$). Moreover, we added a cosine-shaped addition to the model to take care of vasomotion oscillations in the signal during PORH, when seen in the signal. This addition contained extra parameters, such as the amplitude, period, and phase of the oscillation. Those were included as variables in the fits. However, since only a small amount of the measurements showed a significant vasomotion oscillation, we did not further analyze this effect.

### The Iontophoresis Model, with Diffusion and Decay Time Constants

Due to the relatively large contact area of iontophoresis probes (see Figure 4), the iontophoresis process can be considered as a one-dimensional diffusion, with the depth in tissue as a parameter [6] (see Figure 5 and the Appendix). This is in analogy with pharmacological models as used for dermatological purposes. Then, Fick's diffusion law [9] can be used. The diffusion can be described by a characteristic time constant $\tau_{diff}$, the "diffusion time constant," inversely proportional to the diffusion constant. It starts with a gradual increase from zero, not as sharp as in the PORH model, then reaches a maximum at $2\tau_{diff}$ and, finally, decreases toward zero. However, when fitting this simple model, it turned out that the decrease in time was too slow. In analogy again to pharmacokinetic and pharmacodynamic assumptions about metabolism and elimination, and to pharmacodynamic models about saturation and tachyphylaxis, we added an exponentially decreasing decay term. As for the first term, this decay or elimination term also can be described with a time constant $\tau_{decay}$, the "decay time constant," being its initial slope. With this, we again arrive at a model with two characteristic times, such as with the PORH model. Functional comparison of both models (see Appendix) shows that $\tau_{decay}$ will be inversely proportional to the (average) vessel wall thickness or diameter.

Iontophoresis protocols often provide in the administration of multiple shots, shifted in time. We took that into account in the formalism, by summing up the (time-shifted) contributions of all shots with an appropriate factor, the "shot saturation constant" (*SSC*). This constant may vary between 0 (making all shots to contribute equally) and infinity (when the first shot contributes only). It turns out to be an important variable in distinguishing recordings from different types of vasodilators used.

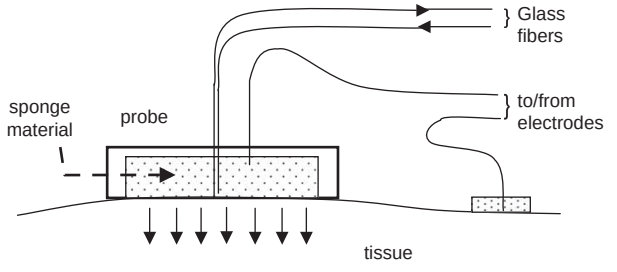


**Figure 4.** Schematic view of an iontophoresis laser-Doppler perfusion flow probe. Dimensions: probe: diameter 12 mm, height 5 mm; fiber separation 250 μm. The diffusion can be considered as monodimensional. The effective area is 110 $mm^2$. The glass fibers provide the transport of laser light to the tissue and the transport of Doppler-shifted scattered light back to the detector.

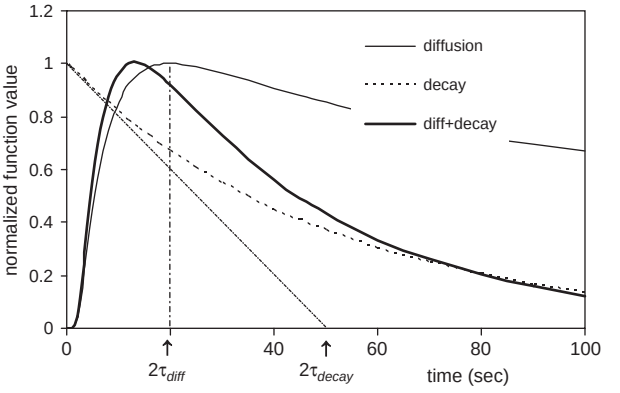


**Figure 5.** The iontophoresis model, as the product of diffusion (time constant $\tau_{diff}$, indicating the top) and decay (time constant $\tau_{decay}$, indicating the initial slope), all normalized to unity. Increasing the time constants causes the functions to broaden.

### The Fitting Process

For the fit of the models to the measurements we used minimization of the reduced chi-squared ($\chi^2$) [7,6]. For an ideal fit, the reduced $\chi^2$, calculated from the standard $\chi^2$ by division by the difference of the number of measured points and the degrees of freedom (the number of model variables), should approach unity as its minimum value.

The fitting program is written in Delphi-Pascal (the executable file is available from the researchers).

## METHODS

Both studies (PORH and iontophoresis) were approved by the local Ethics Committee of the University Medical Center Groningen (Groningen, The Netherlands) and informed consent was obtained from each participant.

### PORH Measurements

The patients with PAOD fulfilled the following in- and exclusion criteria: Fontaine class II–III PAOD, with an ankle-brachial index (ABI) $<0.9$; no diabetes mellitus [excluded greater than six months preceding study according to American Diabetes

Association (ADA) criteria] and no (history of) congestive heart failure; no use of beta-blockers or calcium antagonists or other medication that influences vasomotor tone at least three days before or during the study; and use of aspirin or other thrombocyte aggregation inhibitors except dipyridamol was allowed, as were angiotensin-converting enzyme (ACE) inhibitors, provided the patient was stably instituted. The 10 included PAOD patients (6 males) had a mean age of $61.3 \pm 8.7$ years (range, 49–76). Control patients had no clinical symptoms and signs (foot arteries were palpable) of PAOD, had no diabetes, and were otherwise also healthy. Ten subjects, all male, were included with a mean age of $55.1 \pm 8.1$ years (range, 46–68). Patients with diabetes mellitus (10 subjects, 7 males) all fulfilled the conventional ADA criteria for diabetes, and both type 1 and type 2 patients were included. None of them had symptoms of PAOD, and the ABI was $>0.9$ in all of them. The other exclusion criteria, and medication restrictions, given above for the PAOD patients also apply here. The mean age was $51.7 \pm 6.6$ years (range, 43–63; 7 males).

We used a normal laser-Doppler perfusion flow monitor (Perimed Pf4001; bandwidth 20 Hz to 12 kHz; Perimed AB, Järfälla, Sweden), already available in the clinic, with a custom-made probe with a fiber separation of 250 μm. This instrument measures the perfusion flow in tissue, averaged over directions and depth. A PC equipped with a data-acquisition subsystem recorded the analog outputs of the monitor at a rate of 40 Hz. The data files were processed for conversion from mV to PU (perfusion units) by division with the gain factor of the instrument (10 mV/PU). After, the data were averaged over 40 samples to remove heart-beat fluctuations. This resulted in data at one-second intervals.

All studies were performed in a quiet room with a temperature of $25 \pm 1^0$C, with subjects in a supine position, with the dorsum of the foot at 10 cm above heart level, and a blanket covering the legs up to the ankles. Thirty minutes were taken for acclimatization. For the PORH studies, an 18-cm-wide automatically inflatable cuff (rapid cuff inflator E-20 and air source AG-101; Hokanson, Bellevue, Washington, USA) was installed around the thigh of the left leg, without clothing between leg skin and cuff. In the PORH patients, the leg with the ABI $<0.9$ was chosen. The laser-Doppler flowmeter (LDF) probe was installed on the dorsum of the ipsilateral foot between the second and third metacarpal radius. Arterial pressure was measured in the arm. The maximum cuff pressure was set 30 mmHg above the systolic arm pressure. Three minutes were used for the occlusion period; in case of severe pain and patient intolerability, at least one minute was used. After relief of the occlusion, a minimum of 15 minutes was recorded.

### Iontophoresis Measurements

From 2003 to 2005, all women who are hospitalized or had been hospitalized in the University Medical Center Groningen for a severe early-onset ($<34$ weeks in gestational age) pre-eclampsia were asked to participate after a detailed explanation of the study and protocol.

Pre-eclampsia was defined, according to the criteria of the International Society for the Study of Hypertension in Pregnancy [3], as the appearance of a diastolic blood pressure (DBP) $\geq 90$ mmHg measured at two occasions at least four hours apart in combination with proteinuria ($\geq 300$ mg/24 hours or 2+ dipstick) developing after a gestational age of 20 weeks in a previously normotensive woman. Women with preexisting hypertension (blood pressure before 20 weeks of gestation $\geq 140/90$ mmHg or using antihypertensive medication), diabetes mellitus, renal disease, pre-eclampsia in a previous pregnancy, or using vasoctive drugs were excluded. A total of 48 Caucasian women participated in the postpartum study, including 25 women with a history of early-onset pre-eclampsia and 23 healthy women with uncomplicated pregnancies. Also, 39 pregnant women participated in the pregnancy study, including 12 pregnant pre-eclamptic patients (PE), 10 pregnant patients with pregnancy-induced hypertension (PIH), and 17 pregnant controls (ZC). All women had singleton pregnancies and were tested during pregnancy until 35 weeks of gestation or between 3 and 11 months postpartum. Information on personal history, including past history of hypertension, diabetes, renal diseases, smoking habits, drug therapy, weight, length, and family history (first degree) relating to premature (in men $<55$ years, in women $<65$) cardiovascular diseases (CVDs), was obtained by means of a questionnaire.

Skin perfusion (defined as flux) and microvascular responses to ACh and SNP were measured, as previously described [15,19], by using a Periflux 4000 laser-Doppler system in combination with a Periflux tissue heater set to 31°C (PF4005, Peritemp; Perimed, Sweden). Participants were seated with

their forearms on a soft pillow at heart level. Caffeine-containing drinks or smoking were not allowed two hours prior to the test. Tissue temperature was recorded during the measurements. A special iontophoresis probe (PF481-2; effective area of 110 $mm^2$ Perimed), containing a thermostatic probe holder, was placed on the dorsal side of the middle phalanx of the third finger. ACh response was measured on the dominant hand, whereas SNP was applied on the nondominant hand [19]. A battery-powered iontophoresis controller (PeriIont 382, Perimed, Sweden) was used to provide a direct current for drug iontophoresis. Iontophoresis allows charged substances to cross the skin by means of a small electrical current without inducing systemic effects. Iontophoresis of ACh induces vascular smooth muscle relaxation indirectly via endothelium-derived relaxing factor(s), whereas SNP, a nitric-oxide donor, evokes vasodilatation by directly increasing cGMP in vascular smooth muscle cells [15,10].

After a baseline recording of 100 seconds at rest (baseline flux), iontophoresis was started by setting time and current strength. ACh (1%, Miochol; IOLAB, Bournonville Pharma, The Hague, The Netherlands) was delivered in seven doses of 0.1 milliamps (mA), using an anodal current for 20 seconds with a 60-second interval between each dose to achieve a plateau phase, whereas SNP (0.1%, dissolved in NaCl 0.9%) was delivered in nine doses of 0.2 mA, using a cathodal current for 20 seconds with a 90-seconds interval between each dose. Five minutes after the final iontophoretic delivery, an arterial occlusion at the upper arm was performed by inflating a blood cuff >30 mmHg suprasystolic for two minutes to determine the biological zero-flux level. This is defined as the nonzero laser-Doppler signal obtained from a tissue in the absence of vascular flow [12]. The measurements were performed sequentially; approximately 10 minutes elapsed between the two measurements. Sitting blood pressure was measured by an automated oscillometric blood-pressure monitor at the end of the examination.

Our iontophoresis protocol was based on previously documented, accepted protocols [15,19]. We performed some iontophoretic measurements by using the solvents of the vasodilatators, mannitol and NaCL 0.9%. These measurements (data not shown) only elicited a minimal to almost no increase in blood flow. Therefore, the responses to ACh and SNP used for further analyses are expressed uncorrected for their respective vehicle response.

## RESULTS

### PORH Measurements

Above, we described the model for the PORH provocation [7]. To the model, the exact physical solution can be approximated by a two-stage solution, with an "arterial" and a "capillary" part. This approximation is fully applicable only when the two parts can be considered as being independent. This is the case when the "arterial" time constant $\tau_{art}$ is much smaller than the "capillary" time constant $\tau_{cap}$. The clinical data show that this is not met with the PAOD patients. The control group has the fastest reaction on the cuff release (for both $\tau$'s), followed by the diabetes patients and, finally, the PAOD patients. $\tau_{cap}$ is always larger than $\tau_{art}$, with almost similar ratios for the PAOD and control groups, but much larger for the diabetes group, which reflects the diminished capillary perfusion. As is shown in the Appendix, a larger time constant may be the result of a thicker vessel wall or (more likely) a smaller diameter.

Since the numbers of participants in the three groups were relatively small, we did not perform a Mann-Whitney test to analyze the correspondence between the three groups. From Figure 7 it is seen that, although the SEM bars were relatively large, still significant differences are suggested. The large error bars were, in most cases, due to relatively deviant measurements with some subjects.

For those subjects (controls and patients) who showed significant vasomotion in the signal, we also included a cosine-shaped vasomotion oscillation superposition in the fit, as indicated in Figure 6. This was done because without accounting for the extra cosine signal, the determination of the maximum time and level of the signal became more difficult.

We used the full model (Equation A1) for the analysis of all measurements. As could be expected, application of the approximated model (Equation A2) was justified in cases where $\tau_{art} << \tau_{cap}$, thus especially for controls. Figure 7 shows the differences in the characteristic time constants over the three groups. Larger time constants correspond to a slower development in time, due to higher flow resistances and/or vessel compliances, the latter related to a lower elasticity modulus. Especially, the groups of PAOD patients and controls show large significant differences. All control subjects show a very rapid, almost instantaneous, increase in flow after releasing the occluding cuff. The characteristic

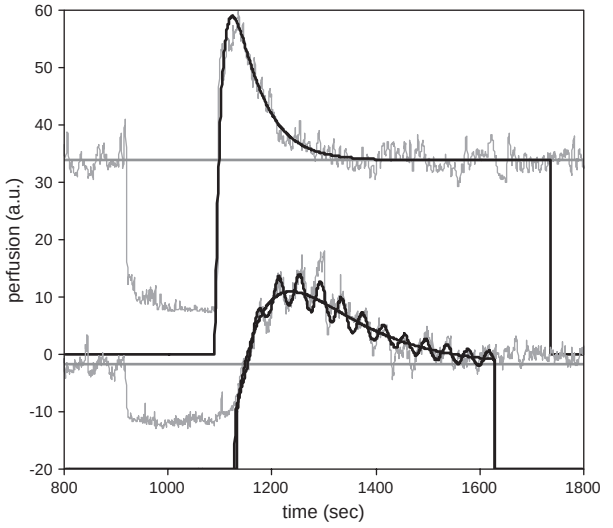


**Figure 6.** Analysis of two typical PORH recordings, from a healthy person (upper) and a PAOD patient (lower). Shown: measurement, resting flux line (with extrapolation) and fitted function, respectively. For clarity, a value of 20 has been subtracted from the lower curves. In the lower figure also, a fit, including vasomotion, is shown. Fits are performed between the vertical lines. Typical differences are: fast vs. slow start after releasing the cuff and fast vs. slow recovery toward normal resting flow values. Parameters for the present recordings: $\tau_{art} = 15$ and 77 seconds; $\tau_{cap} = 52$ and 94 seconds for upper and lower curve, respectively; and vasomotion amplitude and time = 3.3 and 40 seconds, respectively (lower curve only).

time constants of the PAOD group are much longer, probably due to the increase of elasticity (or decrease in Young's elastic modulus) and/or increase in resistance of the arterial and the capillary system, or the disturbed endothelium-dependent vasodilatation in the PAOD group.

We also calculated the ratio of the areas between the measured curve and the extrapolated resting flux line (extrapolated from the time period before occlusion) for the time periods of occlusion and of the PORH response. This ratio of reactive hyperemia area versus occlusion area might indicate how the oxygen debt, created during the occlusion period, is paid off during the reactive hyperemia period. The values show that for healthy persons (the control group) and the PAOD patients, this ratio is below and above unity, respectively. Values for the diabetes mellitus II patients resemble the control group values.

The relative flux overshoot was calculated by using the maximum flux value, derived from the fit of the model, divided by the resting flux level. The controls show a much larger overshoot.

### Iontophoresis Measurements

In Figure 8, we present a typical example of time recordings of two patients. It is seen that upon drug administration, the blood flow increases sharply from the resting-flow level, followed by a much slower decrease toward the resting-flow level. The effect of the multiple shots is clearly seen.

The model was fitted to all 87 recordings of the different groups [12 pregnant pre-eclamptic patients (PE), 10 pregnant patients with pregnancy-induced hypertension (PIH), 17 pregnant controls (ZC), 23 postpartum previously pre-eclamptic women (PPP), and 25 postpartum controls (PPC)], all with both ACh and SNP. The reduced $\chi^2$-values over the five groups for both Ach and SNP measurements are between 1 and 2, indicating fits with deviations from the measured data, ranging from equal to about twice the local standard deviation in those measured data. We may conclude that the fitting procedure worked satisfactorily. Figure 9 shows the results. In this figure, we plotted $\tau_{decay}$ on a logarithmic scale, as discussed below.

Statistical analyses were performed with SPSS software (SPSS Inc., Chicago, Illinois, USA). We used Komolgorov-Smirnov tests to assess the normality of the data. Since parameters turned out to be non-normally distributed, the nonparametric Mann-Whitney test was used for testing group differences [8,20]. For the analysis, we used the SPSS package. Means and their standard deviations, and medians with 25–75% percentiles were calculated. Significance was accepted if $P < 0.05$. For the plots, we choose the medians and percentiles, since most model variables appear in (negative) exponents. Then, large values of those variables are not very distinguishing anymore (e.g., both exp(–1/100) and exp(–1/1,000,000) are very close to unity). This was especially the case for $\tau_{decay}$, which turns out to be sensitive for the exact shape of decrease of the signal after its maximum, and therefore, we present this variable in Figure 9 on a logarithmic scale. Very large $\tau_{decay}$-values are not very distinctive for the fit of the model anymore. It means that the measured data in that time region (after the top), which normally play a large role in the determination of $\tau_{\mathrm{decay}}$, are not very useable for that purpose, sometimes due to large fluctuations in the signal or (in

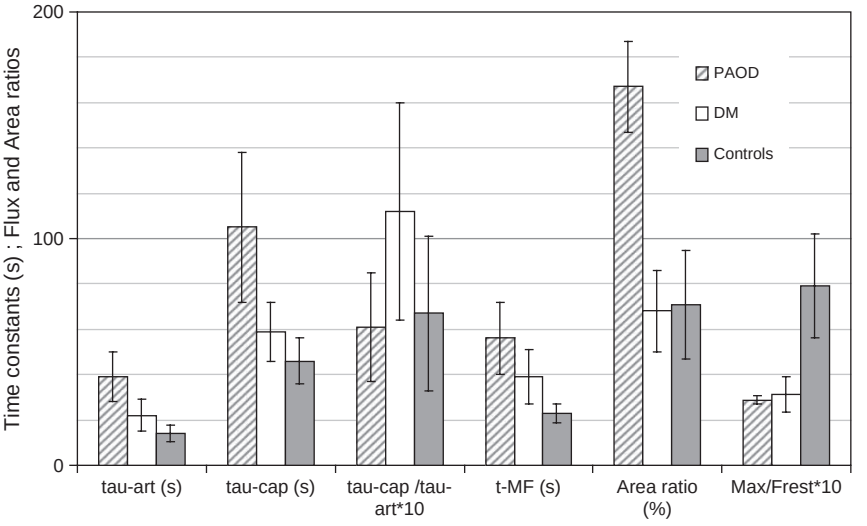


**Figure 7.** Comparison of characteristic times for the three PORH groups, 10 subjects each (left bars: PAOD; middle: diabetes mellitus; right: healthy persons). $\tau_{ar}$ , $\tau_{cap}$ are characteristic times in Equations (A1)–(A2); $t_{MF}$ is the time to the maximum flux value, measured from time of flux increase after cuff release. Also indicated: ratio of areas between measured data and extrapolated resting flux, for reactive hyperemia period versus occlusion period; and: maximum value of the overshoot, divided by the resting flux level. Error bars indicate the SEMs (standard error of the means).

some cases) because the recording had to be stopped prematurely. A similar, but less pronounced, effect was present for *SSC*.

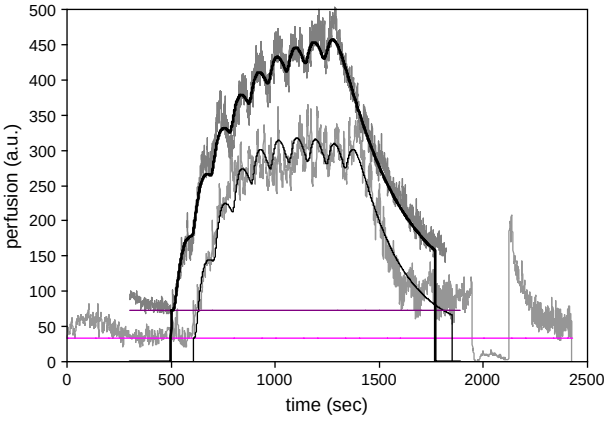


**Figure 8.** Two laser-Doppler iontophoresis recordings of SNP administration, together with their extrapolated resting flux lines and the fitted model. The lower curve also shows an arterial occlusion, performed to obtain the biological zero signal level. Parameters for the present recordings*:* 9 shots with 90-second intervals, $\chi^2_{red} = 1.15$ and 1.90; $\tau_{diff} = 76 \pm 10$ and $65 \pm 12$ seconds; $\tau_{decay} = 408 \pm 30$ and $252 \pm 30$ seconds; $SSC = 0.029 \pm 0.014$ and $0.048 \pm 0.028$ for the upper and lower registration, respectively. The $\chi^2_{red}$ values show that the fit of the upper curve is much better.

## DISCUSSION

### PORH Measurements

From Figure 7 it is seen that the PAOD group has a much slower increase after releasing the cuff than the two other groups (given by $\tau_{art}$) and a much slower return to the resting flux value (given by $\tau_{cap}$). These findings are in agreement with those found in the literature [5,21,13]. This may be interpreted by using an electronic analog (see Appendix), as caused by a decrease in the radius of the vessels. Even assuming that the elasticity of the vessel walls remains comparable, a doubling of the $\tau$'s may well be caused by dividing the vessel radii by two "arterial" or the "capillary" part. This is in agreement with the description of PORH and PAOD, given in the Introduction.

A similar effect is seen in the ratio of the flux overshoot and the resting flux value. Healthy persons frequently show a large overshoot, which can rise to about 10 times the resting flux value, but PAOD patients have a much smaller overshoot, and sometimes the overshoot seems to be almost absent. This indicates that the resistance of the arterial part is that high, that both arteries and capillaries are very slowly filled after an occlusion.

The area ratio indicates the ratio between the areas of the difference of the measured flux and the extrapolated resting flux, between the overshoot

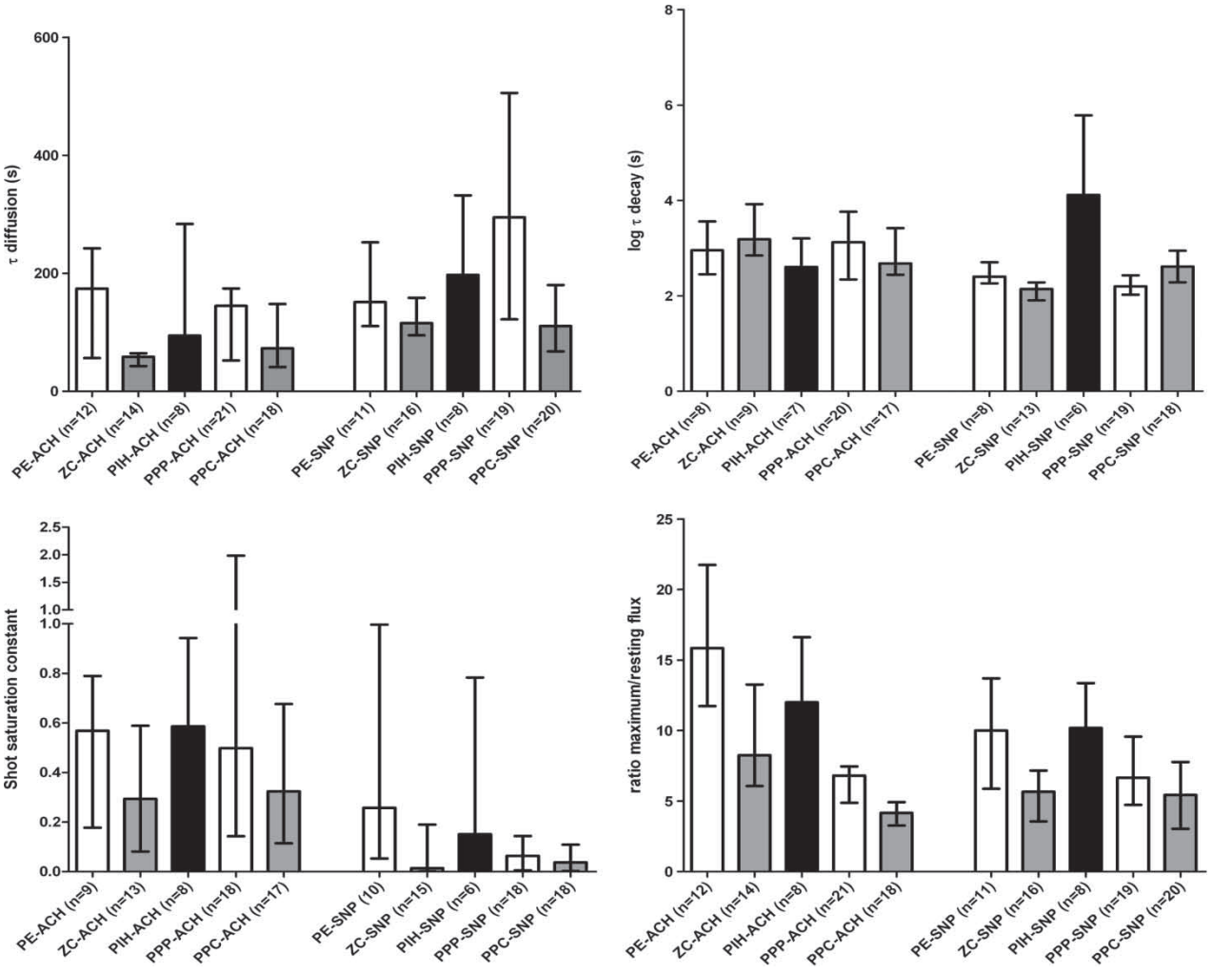


**Figure 9.** Averaged parameter values (diffusion and decay time constants, ratio of maximum flux and resting flux, and shot saturation constant) over the 10 groups of subjects: *PE*, pre-eclamptic; *ZC*, pregnant controls; *PIH*, pregnant, only hypertension; *PPC*, postpartum controls; *PPP*, postpartum patients. Shown: medians with 25 and 75% percentiles (i.e., "error bars"). $\tau_{decay}$ is plotted on a logarithmic scale (for explanation see text).

region and the occlusion region in the signal. This ratio of reactive hyperemia versus occlusion might indicate how the oxygen debt, created during the occlusion period, is paid off during the reactive hyperemia period. For DM and healthy persons (the control group) and for the PAOD patients, this ratio is below and above unity, respectively. This point needs further investigation.

Values for the DM (diabetes mellitus) patients resemble the control group values, except for the maximum/resting flux value, for which values are comparable with those of the PAOD group. This means that perfusion may still react relatively fast on disturbances, but the amount of (overshoot) perfusion is much lower than in normal cases. This might be connected to a "capillary" effect, rather than an "arterial effect," contrary to the PAOD group.

### Iontophoresis Measurements

An overview of all subjects shows that most resulting parameter values are in the same range. However, some of them, especially for $\tau_{decay}$ and for *SSC*, are much higher than the respective medians and thus give the 75% percentiles relatively high values. This is caused by the exponential character of the model, as explained above. Therefore, some values of $\tau_{decay}$ and *SSC*, larger than a preset value of typically $10^5$ and $10^4$ seconds, respectively, are left out of the calculations of these variables (in each group 1 or 2).

Higher values for the time constants indicate a slower time development, slower diffusion, or slower decay (e.g., "washout").

### Diffusion Time Constant $\tau_{diff}$

*Measurements Performed during Pregnancy.* With respect to both Ach and SNP measurements, significant differences can be demonstrated for $\tau_{diff}$ in the three groups using analysis of variance (ANOVA) testing. Post-hoc Dunn analyses [8], [20] demonstrate that for both Ach and SNP, $\tau_{diff}$ is higher in the PE and PIH groups, compared to the control group. Since $\tau_{diff}$ is inversely proportional to the diffusion constant, this indicates a slower diffusion in both hypertensive groups. We hypothesize that this can be accounted for by the common presence of peripheral edema in both PE and PIH patients.

*Measurements Performed 3–13 Months Postpartum.* The diffusion time constant, $\tau_{diff}$, is higher for both the vasodilators Ach and SNP in the formerly pre-eclamptic group. Statistical significant differences could only be found for the SNP measurements.

### Decay Time Constant $\tau_{decay}$

The number of measurements that could be included for the analysis of $\tau_{decay}$ is significantly lower, in comparison to the other parameters. The time interval needed to calculate $\tau_{decay}$ was, in most cases, too short for calculation. In general, a trend of slower decay of ACh is seen for all five groups, in comparison to SNP, indicating that ACh washes out more slowly.

### Ratio Maximum/Resting Flux

*Measurements Performed during Pregnancy.* Significant differences within the pregnancy groups could be demonstrated by ANOVA for both ACh and SNP. Post-hoc Dunn testing [8,20] showed that only the difference between the PE and ZC groups was statistically significant.

*Measurements Performed 3–13 Months Postpartum.* The ratio of ACh was significantly higher in women who had had a pre-eclampsia, in comparison to women who had a normal pregnancy.

### Shot Saturation Constant SSC

The shot saturation constant, *SSC*, is large for ACh but small for SNP. This means that with SNP, all shots do contribute, but that with Ach, only the first (few) shots contribute. However, this effect might be related to the choice of the amount of administered drug, but also to the indirect biological effects of Ach, which is no vasodilator by itself, but acts by inducing endothelial NO release. This point has to be investigated further.

A primary analysis of the microvascular measurements, based on the ratio of maximum and resting flux, has been presented by Blaauw et al. [2], which demonstrated this increased response to ACh in formerly pre-eclamptic patients. Using the model, we are able to add data about the time constants for diffusion and decay, $\tau_{diff}$ and $\tau_{decay}$, respectively, the saturation constant *SSC*, maximum flux, vasodilatation expressed as relative increase in flux from the resting flux obtained by the model, and the time interval from start of the iontophoresis and time of reaching maximum flux.

## CONCLUSIONS

We investigated the dynamics of LDPM signals using (physical) models with time constants, based on (patho)physiological assumptions. This approach renders new information about the dynamics of the reaction of the microcirculation upon provocations such as PORH and iontophoresis. It does not suffer from the inherent difficulties encountered when analyzing the LDPM signal strengths only: lack of absoluteness and conclusiveness. The approach is independent of the instrument used.

We showed that by using a simple two-stage model with two characteristic time constants for the PORH reaction, we can explain differences in the recordings between groups of PAOD and DM patients and healthy persons. The model provides a convenient way to calculate characteristic values of times and signal strengths, which is of great importance when comparing recordings of individual persons or groups. Also for the iontophoresis measurements, we found that a similar two-stage model is appropriate. This model is based on diffusion and decay (or removal) and also accounts for the actual number of contributing shots.

The two characteristic time constants provide convenient equipment to describe the flow dynamics.

The time constants are not dependent upon patient-to-patient differences in signal strengths or upon experimental circumstances. Therefore, we would like to propose these models of two time constants as a method toward quantification of laser-Doppler perfusion signals, to enable interpersonal comparisons, even with different instruments or between different researchers. The models may transform the, so far, limited use of LDPM measurements in clinical practice and provide a more convenient clinical tool.

## ACKNOWLEDGEMENTS

The authors express their thanks to R. Graaff and F. Morales for their valuable discussions and remarks and for making part of their measurements available.

***Declaration of interest:*** The authors report no financial conflicts of interest. The authors alone are responsible for the content and writing of this paper.

## REFERENCES

1. Banga AK. (1998). *Electrically Assisted Transdermal and Topical Drug Delivery*. London: Taylor & Francis.
2. Blaauw J, Graaff R, van Pampus MG, van Doormaal JJ, Smit AJ, Rakhorst G, Aarnoudse JG. (2005). Abnormal endothelium-dependent microvascular reactivity in recently pre-eclamptic women. *Obstet Gynaecol* 105:626–632.
3. Davey DA, MacGillivray I. (1988). The classification and definition of the hypertensive disorders of pregnancy. *Am J Obstet Gynecol* 158:892–898.
4. Davis KR, Ponnampalam J, Hayman R, Baker PN, Arulkumaran S, Donnelly R. (2001). Microvascular vasodilator response to acetylcholine is increased in women with preeclampsia. *BJOG* 108:610–661.
5. Del Guercio R, Leonardo G, Arpaia MR. (1986). Evaluation of postischemic hyperemia on the skin using laser Doppler velocimetry: study on patients with claudicatio intermittens. *Microvasc Res* 32: 289–299.
6. de Mul FFM, Blaauw J, Aarnoudse JG, Rakhorst G. (2007). A diffusion model for iontophoresis measured by laser-Doppler perfusion flowmetry, applied to normal and pre-eclamptic pregnancies. *J Biomed Optics* 12:014032.
7. de Mul FFM, Morales F, Smit AJ, Graaff R. (2005). A model for post-occlusive reactive hyperemia as measured with laser-Doppler perfusion monitoring. *IEEE Trans Biomed Eng* 52:184–190.
8. Dunn OJ. (1964). Multiple comparisons using range sums. *Technometrics* 6:241–252.
9. Fick A. (1855). About diffusion. *Ann Phys Chem Leipzig* 94:59.
10. Furchgott RF, Zawadzki JV. (1980). The obligatory role of endothelial cells in the relaxation of arterial smooth muscle by acetylcholine. *Nature* 288: 373–376.
11. Karnafel W, Juskowa J, Maniewski R, Liebert A, Janik M, Zbiec A. (2002). Microcirculation in the diabetic foot as measured by a multichannel laser Doppler instrument. *Med Sci Monit* 8:137–144.
12. Kernick DP, Tooke JE, Shore AC. (1999). The biological zero signal in laser Doppler fluximetry—origins and practical implications. *Pflugers Arch* 437:624–631.
13. Kvernebo K, Slasgsvold CE, Stranden E. (1989). Laser Doppler flowmetry in evaluation of skin post-ischaemic reactive hyperemia. A study in healthy volunteers and atherosclerotic patients. *J Cardiovasc Surg (Torino)* 30:70–75.
14. Morales F, Graaff R, Smit AJ, Bertuglia S, Petouchova A, Steenbergen W, Léger P, Rakhorst G. (2005). How to assess postocclusive reactive hyperemia by means of laser Doppler perfusion monitoring: application of a standardized protocol to patients with peripheral arterial obstructive disease. *Microvasc Res* 69:17–23.
15. Morris SJ, Shore AC. (1996). Skin blood flow responses to the iontophoresis of acetylcholine and sodium nitroprusside in man: possible mechanisms. *J Physiol* 496:531–542.
16. Morris SJ, Shore AC, Tooke JE. (1995). Responses of the skin microcirculation to acetylcholine and sodium nitroprusside in patients with NIDDM. *Diabetologia* 38:1337–1344.
17. Nilsson GE. (1984). Signal processor for laser Doppler tissue flowmeters. *Med Biolog Eng Compu* 22:343–348.
18. Ryan TJ. (1973). Structure and shape of blood vessels of the skin. In: Jarret A, ed. *The Physiology and Pathophysiology of the Skin* (pp. 577–625). London/New York: Academic Press.
19. Serne EH, Stehouwer CD, ter Maaten JC, ter Wee PM, Rauwerda JA, Donker AJ, et al. (1999). Microvascular function relates to insulin sensitivity and

blood pressure in normal subjects. *Circulation* 99:896–902.
20. Siegel S, Castellan NJ. (1988). Nonparametric Statistics for Behavioural Sciences, 2nd ed. London: McGrawHill.
21. Wahlberg E, Olofsson P, Swedenborg J, Fagrell B. (1992). Effects of local hyperemia and edema on the biological zero in laser Doppler fluxmetry (LD). *Int J Microcirc Clin Exp* 11:157–165.

This paper was first published online on iFirst on 29 May 2009.

## Supplementary Material

## Appendix

The two physical/mathematical models were:

a) PORH flow: Here, we have two time constants [7] (see Figure 3):

$$F = F_{rest}\left[1 - \rho_M.\exp(-\frac{t}{\tau_{art}}) + (\rho_M - 1).\exp(-\frac{t}{\tau_{cap}})\right]. \quad \text{(A1)}$$

with $F_{rest}$ as the resting flux signal, and $\rho_M$ as a factor accounting for the signal intensity. In case the arterial part develops much faster than the capillary part ($\tau_{art} << \tau_{cap}$), this model can be approximated by:

$$F = F_{,rest}\left[1 - \exp(-\frac{t}{\tau_{art}})\right] \times \left[1 + (\rho_M - 1).\exp(-\frac{t}{\tau_{cap}})\right], \quad \text{(A2)}$$

in which the ''arterial'' and ''capillary'' parts can be clearly recognized.

If $\rho_M = 0$, no hyperemia is present, and the flow returns monotonically to the resting flux value.

From a physical point of view, both $\tau$'s can be described in terms of flow resistances $R$ and compliances $C$, and each turns out to be proportional to an effective $RC$ value for the corresponding vessels:

$$\tau \sim R.C = \frac{8\mu l}{\pi R_o^4}.\frac{3\pi R_0^3}{2Eh} = \frac{12\mu l}{EhR_0}$$

where $\mu$ is the blood viscosity, $l$ and $R_0$ are the effective length and radius of the vessels, $h$ is the wall thickness, and $E$ is Young's elastic modulus, proportional to stiffness. Then, a large $\tau$-value corresponds with a small radius or a small stiffness. Since the latter is not likely the case with PAOD patients, a smaller radius (due to obstructions) might be the main cause of slow perfusion.

b) Iontophoresis: Here, we have a diffusion term and a decay term [6] (see Figure 5):

$$\Delta F = \sum_{n=1}^{N} \exp[-(n-1).SSC] \times \frac{C}{\sqrt{t_n}} \exp\left[-\frac{\tau_{diff}}{t_n} - \frac{t_n}{\tau_{decay}}\right]; \quad \text{(A3)}$$

with $\Delta F$ as the excess flux signal and $C$ as an intensity constant. The $n$-summation runs over $N$ shots. Time $t_n$ accounts for the time shift $\Delta t$ between subsequent shots: $t_n = t - (n-1)\Delta t$, with $t$ = time after the start of the first shot.

If the shot saturation constant $SSC = 0$, all $N$ shots contribute equally, and if $SSC >> 1$, the first shot contributes only.

The parameter, $\tau_{diff}$, is inversely proportional to the diffusion constant $D$ (in $m^2/s$), and $\tau_{decay}$ is proportional to the half-lifetime of the decay. Functional comparison of this model with the PORH model shows that $\tau_{decay}$ plays a similar functional role as $\tau_{art}$ and $\tau_{cap}$ and, therefore, will be inversely proportional to the (average) thickness or diameter of the vessel walls.